International Journal of Advances in Applied Sciences (IJAAS)
Vol. 15, No. 1, March 2026, pp. 355∼371
ISSN: 2252-8814, DOI: 10.11591/ijaas.v15.i1.pp355-371

State evolution approach for the axion conversion probability in magnetosphere of a neutron star

Bilal Ahmad[1], Shehreyar Ali[2]
[1]Institute of Theoretical Physics, School of Physics and Optoelectronic Engineering, Beijing University of Technology, Beijing, China
[2]Department of Physics, Govt Degree College No 2 Mardan, affiliated to Abdul Wali Khan University Mardan, Mardan, Pakistan

Article Info

Article history:

Received Jun 12, 2025
Revised Nov. 24, 2025
Accepted Jan 1, 2026

Keywords:

Axion dark matter
Axion-photon conversion
Magnetospheres
Neutron star
Primakoff effect
Radiative power
State evolution

ABSTRACT

Neutron stars (NS), with their extreme gravitational and magnetic fields, provide an exceptional astrophysical laboratory for studying axion dark matter (DM). Through the Primakoff effect, axions can convert into photons within the magnetospheres of NS, a process that may produce observable radio and X-ray signals. In this work, we investigate axion-photon conversion using a novel, time-dependent state evolution formalism, moving beyond the commonly used stationary-path approximations. We derive a generic analytical expression for the conversion probability and calculate the associated radiated power. Our analysis demonstrates that this approach allows NS to strongly constrain the axion-photon coupling constant, reaching sensitivities of $g_{a\gamma\gamma} \simeq \left(10^{-14} - 10^{-15}\right)\ \mathrm{GeV}^{-1}$ for axion masses of $m_a \simeq \left(10^{-3} - 10^{-10}\right)$ eV. These results establish a new pathway to constrain $g_{a\gamma}$ via NS observations. Future campaigns using powerful observatories like the James Webb Space Telescope (JWST), Green Bank Telescope (GBT), and More Karoo Array Telescope (MeerKAT) array will be ideally suited to probe the distinct spectral signatures predicted by our model across multiple frequency domains.

Corresponding Author:

Bilal Ahmad
Institute of Theoretical Physics, School of Physics and Optoelectronic Engineering
Beijing University of Technology
Beijing, China
Email: bilalahmad@emails.bjut.edu.cn

1. INTRODUCTION

The standard model (SM) stands as one of the greatest accomplishments in modern particle physics [1]. Despite its success in predicting the outcomes of terrestrial experiments, it is considered incomplete due to certain problems, including the strong charge parity (CP) problem and dark matter (DM). In the late 1970s, to resolve the strong CP problem in quantum chromodynamics (QCD) by an additional term was introduced in the QCD Lagrangian. It arises from the Peccei-Quinn mechanism [1], which dynamically restores CP symmetry in strong interactions; later, Wilczek and Weinberg [2], [3] assigned the axion as a physical outcome of the spontaneous breaking of $U(1)_{PQ}$ symmetry from Noether's theorem [2]. Hooft [4] studied one of the most important breaks down of $U_{\mathrm{PQ}}(1)$ symmetry is possible due to the Instanton effects, it means that the axion field couples to the gluons field and acts as a shift symmetry i.e. $a(x,t) \rightarrow a(x,t) + \epsilon(x,t)$. Extremely light and weakly interacting, axions are also compelling candidates for DM [5]. Theoretical models beyond the SM, like string theory at low energies, often feature generic pseudoscalars in abundance [4]. While there will exist significant differences between the two environments, the emergent properties of the axion will also be broadly

universal, and an easily characterizable theoretical benchmark will follow [6]. This new particle is a possible candidate to explain the DM content of the universe [7]. Under $U_{\mathrm{PQ}}(1)$ symmetry (axion field), we can write the effective field Lagrangian for QCD theory.

$$\mathcal{L}_{\mathrm{a}} = \mathcal{L}_{\mathrm{QCD}} + \frac{g_s^2}{32\pi}\bar{\theta}\, G^{\mathrm{b}}_{\mu\nu} G^{\mathrm{b}\,\mu\nu} + \frac{g_{\mathrm{s}}^2}{32\pi^2}\left(\frac{\mathrm{a}}{f_{\mathrm{a}}/N}\right) G^{\mathrm{b}}_{\mu\nu}\tilde{G}^{\mathrm{b}\,\mu\nu} \tag{1}$$

Here, f_{a} is the axion decay constant, b stands for the color charge on gluons, and dots represent another possible term in the given Lagrangian, and the second and third show the axion coupling with the gluon field. In the original model for the axion N in Peccei-Quinn–Weinberg–Wilczek model (PQWW), it becomes $N = 6$, we can write as like $N = \sum_f X_f$ and represent color anomaly in $U_{\mathrm{PQ}}(1)$ symmetry, the sum of PQ charges X_f over the fermions in the theory.

The remnants of supernova explosions represent one of the most extreme environments in the universe [8]. These compact objects possess powerful gravitational fields, ultra-dense cores, and some of the strongest magnetic fields known, often exceeding 10^8G to 10^{15}G (from 10^4T to 10^{12}T) [9], [10], in the case of magnetars, from 10^{15}G reaching up to 10^{19}G (from 10^{11}T to 10^{15}T) for more information visit [11]. Such extreme conditions make neutron stars (NS) unique astrophysical laboratories for probing fundamental physics, particularly the behavior of exotic particles like axions. NS are natural sources for axions and environments where these particles can leave observable imprints. Axions can be produced in the dense interiors of NS through various mechanisms, such as nucleon-nucleon bremsstrahlung. For more details, visit [12], [13], and pionic processes are studied by [14]. Once produced, these axions can escape the star due to their weak interactions, carrying away energy and contributing to the cooling of the NS. This energy loss mechanism has been extensively studied and provides stringent constraints on axion properties, such as their coupling strength to matter and their mass. Moreover, the dense magnetized plasma surrounding NS offers a unique setting for axion-photon conversion, a process that could lead to detectable electromagnetic signals.

The electrodynamics of the axion, in terms of Chern-Simons coupling $\mathcal{L} \supset \alpha/8\pi f_{\mathrm{a}} F_{\mu\nu}\tilde{F}^{\mu\nu}$ [15], creates a rich electrodynamical structure in which mixing between axions and photons in external $\vec{E}\cdot\vec{B}$ enables resonant conversion processes. That such an interaction, in terms of axion-improved Maxwell's equations, yields magnetized birefringence, photon-axion spectral splitting in plasmas, and stimulated decays in astrophysical settings, is predicted. In the vicinity of a NS, the intense magnetic fields facilitate this conversion via the Primakoff effect and are explored further by [16], enabling axions to transform into observable photons. Axion-photon conversion is not limited to the immediate vicinity of NS. Axions produced in the core can form dense clouds around the star due to gravitational attraction, and the influence of the magnetic field is explored [17], [18]. These axion clouds, which grow over time, provide an additional reservoir for photon production. The density and spatial distribution of the axion cloud depend on factors such as the NS's magnetic field strength, rotation rate, and age. Observations of anomalous X-ray or radio emissions from NS could thus serve as indirect evidence for axion clouds and their conversion into photons. Diagonalization in an anisotropic environment for coupled axion-photon motion reveals a mixture of polarization states with eigenvalues sensitive to plasma frequency ω_{p} and coupling between axions and photons $g_{\mathrm{a}\gamma\gamma}$. Non-perturbative computations in lattices specify, in addition, photon-emitting topological defects in ALP fields, with new signatures in NS magnetospheres and NS binaries.

Axion DM with its μeV mass and weak couplings to SM fields is avoided in conventional models [19]. Beyond their role in axion-photon conversion, NS also serve as potential sources of axion DM. In the early universe, axions could have been produced non-thermally through mechanisms such as the misalignment mechanism. For more information, see [20], and for string decay, visit [21], leading to a cold and diffuse background of axion DM. NS, with their strong gravitational fields, can capture and accumulate these ambient axions, further enhancing their local density. This accumulation not only amplifies the potential for axion-photon conversion but also provides a unique opportunity to probe the properties of axion DM through astrophysical observations. It is exclusively produced through non-thermal processes such as vacuum misalignment and decay of cosmological topological defects. The misalignment mechanism, with its timescale determined by θ_i and of the axion field during an expanding universe, creates coherent oscillation that redshifts as cold DM. In a key feature, the dynamically linked axion mass m_a to QCD topological susceptibility $m_{\mathrm{a}} \sim \Lambda^2_{\mathrm{QCD}}/f_{\mathrm{a}}$, has its origin in f_{a} the decay constant of the axion, a relation fixing the axions parameter space to both cosmology and high-energy physics. Ringwald and Saikawa [22] studied the axion field dynamics after inflation and this study is also present [23], Peccei-Quinn (PQ) symmetry breaking creates

axionic strings study are discussed [24], [25] and domain walls [26], whose decay puts entropy in the density field of axions, and such breakings during [27] inflation remove inhomogeneities, leaving θ_i a stochastic variable under anthropic selection. Cosmic inflation and such dynamics become intertwined, and isocurvature perturbations with constraints under Planck, tie the abundance of the axion with inflation's Hubble scale $H_{\rm inf}$ and tensor-to-scalar ratio r.

Beyond their role in electromagnetic signatures, axions also impact the thermal evolution of NS. Axion emission through processes like $n + n \rightarrow n + n + a$ contributes to cooling, particularly in young NS where the core temperature is high. However, this cooling effect diminishes over time as neutrino and photon emissions [28] dominate in older stars. Observations of NS cooling, such as those of the Cassiopeia A supernova remnant [29], have been used to constrain axion properties, although uncertainties in microphysics complicate the interpretation of data. Overall, the study of axion electrodynamics in NS backgrounds offers profound insights into fundamental physics, bridging particle physics, astrophysics, and cosmology, while providing a promising avenue for indirect axion detection.

The study of axion-photon conversion in NS environments is a rapidly evolving field, driven by advances in observational techniques and theoretical modeling. Noordhuis *et al.* [30] have explored the implications of axion clouds for NS observables, including their cooling rates, spin-down behavior, and electromagnetic emissions. For instance, detecting anomalous X-ray or gamma-ray signals from NS could provide direct evidence for axion-photon conversion. Similarly, radio observations of NS magnetospheres offer a complementary approach to probing axion properties.

This work distinguishes itself through its core methodological approach. While many studies of axion-photon conversion in NS magnetospheres rely on the Wentzel–Kramers–Brillouin (WKB) approximation or stationary-phase integration along a path [31]–[33], we employ a time-dependent state evolution formalism. This technique, inspired by quantum mechanical two-level systems, solves the coupled equations of motion by diagonalizing the mixing matrix in the time domain. This provides a direct and transparent framework for deriving the conversion probability, which is particularly suited for analyzing coherent evolution over time. The primary novelty of this paper is the derivation of a new analytical expression for the axion-photon conversion probability from this state evolution perspective, and the subsequent demonstration that this approach predicts a radiated power approximately 10^{23} orders of magnitude larger than that estimated from static or propagating-state formalisms [9], from this study, we are sure the cooling rate of NS will be much faster, as already discussed in [34], [35]. The state evolution approach sheds light on fundamental physics and links axion DM with the NS cooling rate, providing a shred of strong evidence for the kilonova signal. We need to consider a multi-directional approach to enhance and gain extra sensitivity in ongoing experiments. In the future, the Green Bank Telescope (GBT) [36], More Karoo Array Telescope (MeerKAT) [37], and James Webb Space Telescope (JWST) [38], [39] projects will explore this region $g_{\rm a\gamma\gamma} \simeq \left(10^{-14} - 10^{-15}\right)\ {\rm GeV}^{-1}$.

The roadmap of this work is as follows: in section 2, we provide a basic overview of ongoing experimental and theoretical limits on the axion-photon coupling constant. In section 3, we discuss axion-photon mixing, state evolution probability, and flux analysis. We discuss the radiative power of axion-photon conversion for state evolution in section 4. In section 5, the result and discussion of this research is presented. Finally, section 6 and 7 present limitation and conclude this work.

2. LITERATURE REVIEW

Noordhuis *et al.* [32] demonstrated that NS can accumulate dense "axion clouds" through non-stationary pair plasma discharges in their polar cap regions, particularly for axion masses in the range $\left(10^{-9} \leq m_{\rm a} \leq 10^{-4}\right)$ eV. These axions remain gravitationally bound and accumulate over astrophysical timescales, reaching densities that can exceed $\mathcal{O}(10^{22})$ GeV cm^{-3}, even for very small axion-photon couplings. The authors show that such clouds dissipate energy primarily via resonant axion-photon conversion in the magnetosphere, producing distinctive radio signatures such as narrow spectral lines and transient bursts. Their work highlights NS as promising laboratories for probing axion-like particles, with potential detectability using current radio telescopes like low-frequency array (LOFAR) [40] and GBT [41]. It underscores the importance of time-dependent and plasma-aware modeling in predicting observable signals.

In a significant advancement of magnetospheric modeling, Miguel [10] developed a comprehensive framework for axion-photon conversion that incorporates both pair multiplicity factors and relativistic plasma effects, moving beyond the traditional Goldreich-Julian density profile [42]. This work demonstrated that

accounting for electromagnetic cascades and charge acceleration in pulsar and magnetar magnetospheres significantly shifts the resonant conversion to higher frequencies, potentially extending detectable signals into the millimeter band for axion masses up to approximately 1 meV. The study identified SGR 1745–2900 as a particularly promising target due to its strong magnetic field and location in the Galactic Center region with enhanced DM density. While this model provides crucial insights into magnetospheric complexities, our work complements it by employing a fundamentally different, time-dependent state evolution approach rather than the stationary-path approximations common in the literature. Miguel [10] focus on how plasma properties affect resonance conditions, we derive a new analytical expression for conversion probability that captures coherent quantum evolution over time, revealing a dramatically enhanced radiated power that could explain rapid NS cooling and provide stronger constraints on axion-photon coupling.

Terças *et al.* [31] investigated impact of resonant axion-plasmon conversion in NS magnetospheres, revealing a significant suppression of detectable radio signals from axion-photon interactions. The authors demonstrate that in dense plasma environments, axions can resonantly convert into longitudinal plasmon modes at a smaller radius $r_{\mathrm{c,p}}$ than the standard axion-photon conversion radius $r_{\mathrm{c},\gamma}$, effectively reducing the photon-production volume. This non-radiative energy loss diminishes the expected flux density reaching Earth, shifting experimental sensitivity curves into regions already excluded by existing constraints. Their findings emphasize the critical need to incorporate plasma collective effects into axion search strategies, as neglecting axion-plasmon interactions may lead to overly optimistic projections for radio-telescope-based detection efforts.

In a complementary approach to magnetospheric conversion, Roy *et al.* [38] investigated the potential of the JWST [43] to detect eV-scale axion DM via its decay into photons within the Milky Way halo. Their work forecasts that JWST's end-of-mission blank-sky observations will provide leading sensitivity to axion-photon couplings $g_{\mathrm{a}\gamma\gamma} \geq 5.5 \times 10^{-12}\,\mathrm{GeV}^{-1}$ for axion masses between 0.18 and $2.6\,\mathrm{eV}$, potentially ruling out nucleophobic QCD axions with masses above approximately $0.2\,\mathrm{eV}$. While their study focuses on the decay of ambient Galactic DM, our work explores a fundamentally different production mechanism: the conversion of axions into photons within the extreme environment of a NS magnetosphere via the Primakoff effect. The two approaches are highly complementary; JWST probes the decay of diffuse axions, whereas our state evolution formalism applied to NS signals is sensitive to the local conversion of axions, potentially from both the ambient halo and those produced or accumulated by the NS itself. Together, these methods cover distinct yet overlapping regions of the axion parameter space, with our predicted sensitivity of $g_{\mathrm{a}\gamma\gamma} \simeq 10^{-15}\,\mathrm{GeV}^{-1}$ for $m_{\mathrm{a}} \simeq 10^{-6}\,\mathrm{eV}$ exploring a different, lower-mass and weaker-coupling regime that is beyond the scope of JWST decay searches but potentially accessible through targeted radio and X-ray observations of NS.

In a direct search for axion DM, Foster *et al.* [36] used the GBT and the Effelsberg 100-m radio telescope to look for the predicted conversion of axions into radio photons within the strong magnetic fields of NS. The search targeted nearby isolated NS and the dense Galactic Center region, scanning the highly motivated axion mass range of approximately $(5-11)\ \mu\mathrm{eV}$ for $(1.1\,\mathrm{to}\,2.7)\ \mathrm{GHz}$. Their analysis, which employed a robust likelihood-based framework to identify ultra-narrow spectral lines, found no significant evidence for an axion signal. Consequently, the study placed some of the most stringent constraints to date on the axion-photon coupling constant $g_{a\gamma\gamma}$ for this mass range, excluding new parameter space beyond previous laboratory experiments and demonstrating the powerful potential of radio telescopes in hunt for particle DM.

In their 2021 study, Witte *et al.* [44] address key theoretical uncertainties in axion DM searches via NS radio signals by developing an end-to-end ray-tracing simulation that incorporates plasma effects within the Goldreich-Julian magnetosphere model [42]. Their analysis reveals several critical phenomena previously overlooked: strong anisotropy in the radio flux, significant spectral line broadening due to photon-plasma interactions, premature axion-photon dephasing from refraction, and time-dependent signal variations influenced by viewing angle and magnetospheric geometry. The authors also highlight that exceptionally strong magnetic fields—such as those of magnetars—can lead to cyclotron absorption, reducing detectability. This work highlights the importance of incorporating plasma dynamics into future axion search strategies and offers a flexible computational framework to mitigate theoretical uncertainties in indirect detection efforts.

This work presents a novel time-domain search for axion DM using radio observations of the pulsar PSR J2144-3933 with the MeerKAT telescope [37]. Unlike previous frequency-domain approaches, the authors employ a matched-filter technique to leverage the predicted time-varying signature of axion-photon conversion in the pulsar's magnetosphere, which arises from its rotating, non-axisymmetric plasma structure. Analyzing

4,416 seconds of data, they find no significant signal and place an upper limit on the axion-photon coupling of $g_{a\gamma} < 5.5 \times 10^{-11}\,\mathrm{GeV}^{-1}$ over the mass range $(3.9 - 4.7)\ \mu\mathrm{eV}$ (assuming a pulsar distance of $0.165\,\mathrm{Kpc}$) and constraints are shown in Figure 1. The study demonstrates that time-domain information can enhance sensitivity compared to time-averaged flux measurements, particularly for NS with large magnetic fields. It also discusses prospects for targets like the Galactic Center Magnetar and next-generation telescopes, such as the square kilometre array (SKA) [45].

The Conseil Européen pour la Recherche Nucléaire (CERN) axion solar telescope (CAST)-center for axion and precision physics research (CAPP) experiment [46], represents a significant advancement in the direct search for galactic DM axions within the mass range of $(19.74 - 22.47)\ \mu\mathrm{eV}$, employing a haloscope composed of four phase-matched resonant cavities operating inside CERN's $8.8\,\mathrm{T}$ dipole magnet. By utilizing a fast frequency tuning mechanism $(10\,\mathrm{MHz/min})$ and coherent signal combination across multiple cavities, the collaboration achieved enhanced sensitivity, collecting data over 4124 hours from 2019 to 2021. The analysis excluded axion-photon couplings down to $g_{a\gamma\gamma} = 8 \times 10^{-14}\,\mathrm{GeV}^{-1}$ at 90% confidence level, probing previously unexplored parameter space, as shown in Figure 2. The experiment also demonstrated novel techniques, such as phase-matching and rapid scanning, that pave the way for future large-scale axion searches, including sensitivity to transient signals from axion streams or mini-clusters.

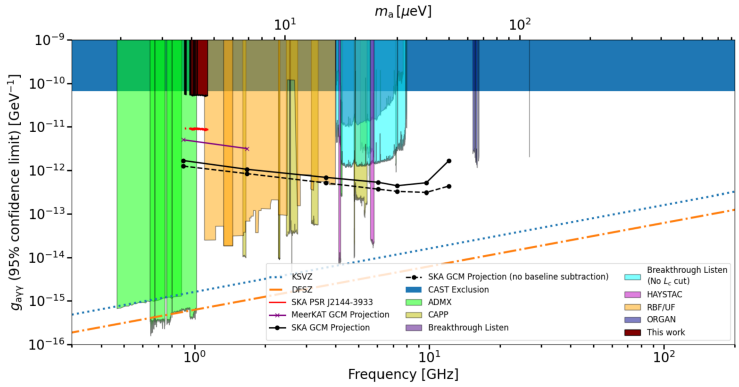

Figure 1. The axion-photon coupling from 1 hour observations of PSR J2144-3933 from the SKA (red) [37]

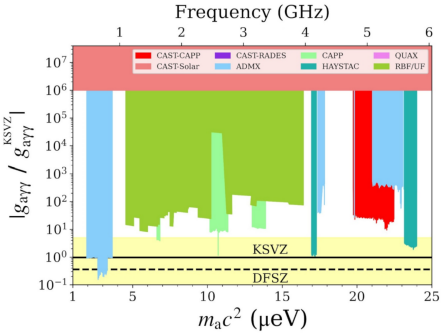

Figure 2. CAST-CAPP, sensitivity on $g_{a\gamma\gamma}$ as a function of axion mass with 95% confidence level [46]

3. METHODS

This work investigates axion-photon conversion in NS magnetospheres using a novel, time-dependent state evolution formalism. This approach provides a distinct and powerful alternative to the commonly employed WKB or stationary-phase approximations [31]–[33]. By framing the problem in the time domain and drawing an analogy to a quantum mechanical two-level system, we directly solve the coupled equations of motion for the axion and photon fields. The core of our methodology involves diagonalizing the axion-photon

mixing matrix to derive a new, generic analytical expression for the conversion probability. This technique is particularly well-suited for capturing the coherent evolution of the system over time, offering a transparent framework that reveals a significantly enhanced radiated power compared to static or propagating-state formalisms, with profound implications for NS cooling rates and observable signals.

3.1. Axion electrodynamics

Axion electrodynamics in the NS background represents a fascinating interplay of particle physics and astrophysics. In this context, axions are hypothetical light pseudo-scalar particles interact with electromagnetic fields in the extreme environments surrounding NS. NS, characterized by its immense gravitational fields, ultra-strong magnetic fields (ranging from 10^{15} G to 10^{19} G in magnetars) [9]–[11], and dense plasma governed by Maxwell's equations as in (2) and (3) [42]. Provide unique conditions for studying axions.

$$\vec{\nabla} \cdot \vec{E} = \rho\,, \quad \vec{\nabla} \times \vec{E} = -\partial_t \vec{B} \tag{2}$$

$$\vec{\nabla} \cdot \vec{B} = 0\,, \quad \vec{\nabla} \times \vec{B} = J + \partial_t \vec{E} \tag{3}$$

3.2. Modified Maxwell's equations for axion dark matter

A set of Maxwell's equations acquired from this approximation exactly describes the reacted fields generated from the axion-photon interaction. This interaction leads to the conversion of axions into photons through the inverse Primakoff effect in the presence of a NS magnetic field [16]. Many of the successful experiments searching for axions rely on this axion-photon coupling, along with the assumption that axions constitute halo DM [15], [47], [48], and are therefore referred to as axion haloscope searches. To account for the axion interaction with electromagnetic fields, classical Maxwell's equations must be modified accordingly. The effective Lagrangian that describes the axion-photon interaction, including an axion-like term, can be derived in system international (SI) units as (4).

$$\mathcal{L}_a = \frac{1}{2}\partial_\nu a \partial^\nu a - \frac{1}{2}m^2 a^2 + \frac{g_{a\gamma}}{4} a F_{\mu\nu}\tilde{F}^{\mu\nu} + \cdots\} \tag{4}$$

Modified Gauss law:

$$\begin{aligned}\partial_\mu F^{\mu\nu} &= g_{a\gamma}\partial_\mu a \tilde{F}^{\mu\nu} + \partial_\mu F^{\mu\nu} \\ &= \frac{1}{2} g_{a\gamma}\epsilon^{\mu\nu\rho\sigma}\partial_\mu a F_{\rho\sigma} + J^\nu\end{aligned}$$

Here, $\frac{1}{2}\epsilon^{\mu\nu\rho\sigma}F_{\rho\sigma}$, if $\nu = 0$ and $\mu = 0, k$, then (5).

$$\partial_i E^i = \frac{1}{2} g_{a\gamma}\vec{\nabla} a \cdot \vec{B} + \rho_a \tag{5}$$

Modified ampere law: after simplification as in (6).

$$\vec{\nabla} \times \vec{B} - \frac{\partial E}{\partial t} = g_{a\gamma}\left(\vec{\nabla} a \times E - \frac{\partial a}{\partial t}\vec{B}\right) + J \tag{6}$$

Modified Faraday law: as we know the duality transformation of the $\vec{E}$ and $\vec{B}$, hold equally with asymmetric nature, after doing transformation in (6), in result we get (7).

$$\vec{\nabla} \times \vec{E} + \frac{\partial \vec{B}}{\partial t} = -g_{a\gamma}\left(\vec{\nabla} a \times \vec{B} + \frac{\partial a}{\partial t}\vec{E}\right) + J \tag{7}$$

Equation of motion for $\vec{E}$ and $\vec{B}$ fields: let's use (8).

$$\left(\vec{\nabla} \times \vec{B}\right) = \partial_t \vec{E} - g_{a\gamma}\left(\vec{E} \times \vec{\nabla} a - \vec{B}\partial_t a\right) \tag{8}$$

Now taking curl of $\left(\vec{\nabla} \times \vec{B}\right)$, then we get (9).

$$\vec{\nabla} \times \left(\vec{\nabla} \times \vec{B}\right) = \vec{\nabla} \times \left(\partial_t \vec{E}\right) - g_{a\gamma}\vec{\nabla} \times \left(\vec{E} \times \vec{\nabla} a - \vec{B}\partial_t a\right) \tag{9}$$

After using vector identities,

$$\nabla^2\vec{B}+\partial_t^2\vec{B}=-g_{a\gamma}\vec{E}\left(\vec{\nabla}\cdot\vec{\nabla}a\right)-g_{a\gamma}\vec{\nabla}a\left(\vec{\nabla}\cdot\vec{E}\right)+g_{a\gamma}\left(\vec{\nabla}a\cdot\vec{\nabla}\right)\vec{E}-g_{a\gamma}\left(\vec{E}\cdot\nabla\right)\vec{\nabla}a + g_{a\gamma}\left[\vec{\nabla}\left(\partial_t a\right)\times\vec{B}+\partial_t a\left(\vec{\nabla}\times\vec{B}\right)\right]$$

Simplified form for $\vec{B}$-field, using Coulomb gauge $\partial_\mu\nabla^\mu=0$ as in (10).

$$\nabla^2\vec{B}-\partial_t^2\vec{B}=-g_{a\gamma}\partial_t\vec{E}\partial_t a \tag{10}$$

Similarly equation of motion for $\vec{E}$ field will be (11).

$$\vec{\nabla}^2\vec{E}-\partial_t^2\vec{E}=g_{a\gamma}\partial_t\vec{B}\partial_t a \tag{11}$$

Equation of motion for axion and photon fields: from classical field theory, we can write the action for the axion field as (12).

$$S=\int d^4x\left[-\frac{1}{2}\left(\partial_\mu a\partial^\mu a+m_a^2a^2\right)-\frac{1}{4}g_{a\gamma\gamma}aF_{\mu\nu}\tilde{F^{\mu\nu}}\right] \tag{12}$$

Let's equate the interaction terms set to zero. Using the KG-wave equation for the axion field as in (13).

$$-\frac{1}{2}\left(\partial_\mu a\partial^\mu a+m_a^2a^2\right)=\Box a+m_a^2a \tag{13}$$

After simplifications, the result equation of motion will be (14).

$$\Box a+m_{\rm a}^2a=-g_{\rm a\gamma\gamma}\vec{E}\cdot\vec{B}_{\rm n} \tag{14}$$

The term $\vec{E}\cdot\vec{B}_{\rm n}$ represents the EM component and comes from the axion-photon interaction. In astrophysical environments like NS magnetospheres, regions with non-zero $\vec{E}\cdot\vec{B}_{\rm n}$ (e.g., due to dynamical screening in vacuum gaps) can efficiently produce axions where axion mixed with $\vec{E}\cdot\vec{B}_{\rm n}$ and photon equation of motion as in (15).

$$\Box A=g_{\rm a\gamma\gamma}\partial_t a\vec{B}_{\rm n} \tag{15}$$

The dispersion relation of a photon in a plasma is (16).

$$\omega^2-k^2\simeq\omega_{\rm p}\,,\quad \omega_{\rm p}=\sqrt{\frac{4\pi\alpha n_{\rm e}}{m_{\rm e}}} \tag{16}$$

Here, $\omega_{\rm p}$ is plasma frequency, $n_{\rm e}$ electron number density, and α is the fine-structure constant. In general, $\omega_{\rm p}=1.31\times10^{18}\sqrt{n_{\rm e}/10^{26}\,{\rm cm}^{-3}}R_\odot^{-1}$, here $R_\odot$ is solar radius.

3.3. The mixing of axion-photon fields

Axion is a very elusive particle that only interacts via gravitational interaction, the detection of the axion is tricky so the detection of axion can be probed via the conversion of the photon into axion and vice versa, as occurs in the sun which is known as Primakoff conversion [49], this process is the key phenomenon through which any neutral particle can be converted into two photons in the presence of columbic field of the nucleus. Similarly, the axion can be converted into two photons in the presence of an external electromagnetic field, which influences the conversion phenomenon. In any experiment, the conversion of the axion into a photon can happen statistically, which can be predicted through the probability of the conversion of the axion into a photon. In this work, we will explore the conversion probability of axions into photons in the presence of a NS magnetic field, utilizing the axion-photon mixing mechanism. In astrophysical environments such as NS, axions can be produced through processes like nucleon-nucleon bremsstrahlung in dense nuclear matter and can couple to photons via the axion-photon interaction term. This coupling facilitates processes such as the Primakoff effect, where axions convert into photons in the presence of strong magnetic fields. As a result, the magnetospheres of NS provide ideal environments for detecting axion-induced signals.

Axion converts into photons in the presence of a NS magnetic field $\vec{B}_n$, which could be dubbed as an oscillation of axion into photons. We did our analysis in the time domain oscillation instead of the spatial

component because, in NS magnetospheres, the magnetic field and plasma density can change over time due to processes like magneto-rotational spin-down or glitches. These changes affect the axion-photon conversion dynamics, making a time-dependent analysis more appropriate for axion conversion into photons. The plane wave solution for the axion and photon fields is (17) and (18).

$$a\left(\mathrm{r},t\right)=a_0e^{i\vec{k}\mathrm{r}-i\omega t} \tag{17}$$

$$A\left(\mathrm{r},t\right)=A_0e^{i\vec{k}\mathrm{r}-i\omega t} \tag{18}$$

Here, both plane waves satisfy both equation of motion instead of fixing any specific direction we are dealing with in the time domain, because if we fix the axion field oscillation or the photon field propagation in one direction, we might be we lose the friction of data, then as a result we get (19) and (20).

$$\left(\partial_t^2-\vec{k}^2-m_a^2\right)a=-g_{a\gamma\gamma}\omega A\vec{B}_n \tag{19}$$

$$(\partial_t^2-\vec{k}^2)A=-g_{a\gamma\gamma}\omega a\vec{B}_n \tag{20}$$

Now (19) and (20) we can write in matrix form and also use (16), so we get a very simplified form as in (21).

$$\partial_t\left[\begin{array}{c}A\left(t\right)\\a\left(t\right)\end{array}\right]=\left[\begin{array}{cc}-\frac{\omega_{\mathrm{p}}^2}{2\omega} & -\frac{1}{2}g_{a\gamma\gamma}\vec{B}_n\\-\frac{1}{2}g_{a\gamma\gamma}\vec{B}_n & -\frac{m_a^2}{2\omega}\end{array}\right]\left[\begin{array}{c}A\left(t'\right)\\a\left(t'\right)\end{array}\right] \tag{21}$$

Where, ω is photon frequency and m_{a} is axion mass. Here, $\Delta_{a\gamma}=-\frac{1}{2}g_{a\gamma\gamma}\vec{B}_n$, $\Delta_{\mathrm{p}}=-\frac{\omega_{\mathrm{p}}^2}{2\omega}$, and $\Delta_a=-\frac{m_a^2}{2\omega}$, let's substituted back then we get (22).

$$M=\left[\begin{array}{cc}\Delta_{\mathrm{p}} & \Delta_{\mathrm{a}\gamma}\\\Delta_{\mathrm{a}\gamma} & \Delta_{\mathrm{a}}\end{array}\right] \tag{22}$$

3.4. Mathematical modeling

The derivation of the Schrödinger-like evolution in (22) relies on a set of specific physical approximations which we now clarify.

- Linearly polarized photons and constant magnetic field: we consider the conversion of axions into a single dominant polarization mode of the photon, parallel to the external magnetic field $\vec{B}_n$, which is assumed to be constant and homogeneous over the conversion region for this initial derivation. This allows us to treat the photon field as a scalar, A.
- High-energy approximation ($\omega \gg m_a, \omega_p$): we assume the particle energy ω is much larger than both the axion mass m_a and the plasma frequency ω_p. This justifies the use of the relativistic dispersion relation and allows us to approximate the d'Alembert operator as $(\partial_t^2-\nabla^2)\approx 2i\omega(\partial_t+\partial_z)$ for a plane wave $e^{-i\omega t+ikz}$ [50].
- Time-domain focus and forward propagation: we neglect spatial derivatives perpendicular to the propagation direction and focus on the time evolution, effectively considering a localized region of the magnetosphere. This simplifies the problem to a first-order differential equation in time, $\partial_t \approx -i\mathcal{H}$, where $\mathcal{H}$ is the Hamiltonian.
- Neglect of back-reaction: we assume the photon field generated by axion conversion is small and does not significantly back-react on the axion field or the external magnetic field.

We now assume that the mass matrix in (21) is independent of any fixed direction. This implies that the magnetic field remains constant, with a fixed magnitude and direction, and that the conversion occurs in a homogeneous plasma at a constant frequency. Under these conditions, the mass matrix can be diagonalized with $RMR^{\dagger}$, allowing us to transform it unmixedly. Let's solve eigenvalue, since $(M-\lambda I)\,v=0$, then we get eigenvalues, for our case as in (23).

$$\lambda_{\pm}=-\frac{m_{\mathrm{a}}^2+\omega_{\mathrm{p}}^2\pm\sqrt{4\vec{B}_{\mathrm{n}}^2g_{\mathrm{a}\gamma\gamma}^2\omega^2+\left(m_{\mathrm{a}}^2-\omega_{\mathrm{p}}^2\right)^2}}{4\omega} \tag{23}$$

From neutrino oscillation using a mixing angle approach $\tilde{M} = R^T M R$ (24).

$$R = \begin{bmatrix} \cos\theta & \sin\theta \\ -\sin\theta & \cos\theta \end{bmatrix} \tag{24}$$

And R^T is transpose of rotational metrics R. Then, as a result, we get an unmixed matrix for the axion conversion probability as in (25).

$$D = \begin{pmatrix} -\dfrac{m_a^2 + \omega_p^2 + \sqrt{4B^2 g_{a\gamma\gamma}^2 \omega^2 + (m_a^2 - \omega_p^2)^2}}{4\omega} & 0 \\ 0 & -\dfrac{m_a^2 + \omega_p^2 - \sqrt{4B^2 g_{a\gamma\gamma}^2 \omega^2 + (m_a^2 - \omega_p^2)^2}}{4\omega} \end{pmatrix} \tag{25}$$

The matrix D encapsulates the evolution of the axion-photon system from the initial point to an arbitrary point. This solution was derived using the equation of motion given in (25).

3.5. Axion conversion probability

The state evolution tactic in axion-photon mixing offers a powerful background for understanding the time-dependent dynamics of axion-to-photon conversion in systems such as dense astrophysical environments or laboratory experiments. This technique explains the coupled quantum equations of motion (QEoM) for the axion and photon fields, accounting for classical mean-field effects and quantum fluctuations that kernel the instability driving the mixing. By presenting scaled variables and rescaling operators to knob large particle numbers efficiently, the method captures the evolution of photon modes from an initially pure axion state through a "quantum break" mechanism, where coherent axion-photon interactions lead to swift energy transfer. Significantly, this formalism incorporates multi-mode effects, mitigating logarithmic factors related to single-mode approximations, while also addressing challenges like redshift and inhomogeneity by simulating spatially extended systems. The result is a vigorous explanation of how axion clouds evolve into mixed states with significant electromagnetic components, contributing insights into observable signatures such as radio emission or X-ray signals from NS. Let's define a relation for the conversion of axions into photons through state evolution as in (26).

$$P_{a\to\gamma} = \left| \left\langle A\left(t\right) \middle| a\left(t\right) \right\rangle \right|^2 \tag{26}$$

Using [50], [51] and derive, $\left|a\left(t\right)\right\rangle = -\sin\theta \left|a_1(0)\right\rangle + \cos\theta \left|a_2(0)\right\rangle$ and quantum state for photon. After time t when axion field evolves, $\left|A\left(t\right)\right\rangle = \cos\left[\theta\right] e^{-i\lambda_1 t} \left|A_1(0)\right\rangle + \sin\left[\theta\right] e^{-i\lambda_2 t} \left|A_2(0)\right\rangle$. Then (26) will be (27).

$$\begin{aligned} P_{a\to\gamma} = \big| & -e^{-i\lambda_1 t} \sin\left[\theta\right] \cos\left[\theta\right] \left\langle A_1(0)|a_1(0)\right\rangle + e^{-i\lambda_1 t} \cos^2\left[\theta\right] \left\langle A_1(0)|a_2(0)\right\rangle \\ & - e^{-i\lambda_2 t} \sin^2\left[\theta\right] \left\langle A_2(0)|a_1(0)\right\rangle + e^{-i\lambda_2 t} \sin\left[\theta\right] \cos\left[\theta\right] \left\langle A_2(0)|a_2(0)\right\rangle \big|^2 \end{aligned} \tag{27}$$

Using the orthogonality conditions, $\left\langle \phi_i \middle| \phi_j \right\rangle = \delta_{ij}$ and must follow if $i = j$ it should be 1 otherwise 0. Then (27) as in (28).

$$P_{a\to\gamma} = \left|\sin\left[\theta\right] \cos\left[\theta\right] \left(e^{-i\lambda_2 t} - e^{-i\lambda_1 t}\right)\right|^2 \tag{28}$$

Using exponential form of $\sin\left[\theta\right]$, so $e^{-i\lambda_2 t} - e^{-i\lambda_1 t} = -2i \sin\left[\left(\lambda_2 - \lambda_1\right) t/2\right]$. After some straight forward calculation, then our expression will be (29).

$$P_{a\to\gamma} = \sin^2\left[2\theta\right] \sin^2\left[\frac{\left(\lambda_2 - \lambda_1\right) t}{2}\right] \tag{29}$$

Now use eigenvalues expressions, which is $\lambda_1 = -m_{\mathrm{a}}^2 + \omega_{\mathrm{p}}^2 + \sqrt{4\vec{B}_{\mathrm{n}}^2 g_{\mathrm{a}\gamma\gamma}^2 \omega^2 + \left(m_{\mathrm{a}}^2 - \omega_{\mathrm{p}}^2\right)^2}/4\omega$ and $\lambda_2 = -m_{\mathrm{a}}^2 + \omega_{\mathrm{p}}^2 - \sqrt{4\vec{B}_{\mathrm{n}}^2 g_{\mathrm{a}\gamma\gamma}^2 \omega^2 + \left(m_{\mathrm{a}}^2 - \omega_{\mathrm{p}}^2\right)^2}/4\omega$, and solve with the basic algebraic approach then the result of eigenvalues difference is $\Delta_{\mathrm{eff}} = \lambda_2 - \lambda_1 = \sqrt{4\vec{B}_{\mathrm{n}}^2 g_{\mathrm{a}\gamma\gamma}^2 \omega^2 + \left(m_{\mathrm{a}}^2 - \omega_{\mathrm{p}}^2\right)^2}/2\omega$ and from here [50], [51], we can write a relation for $\sin[2\theta]$ as in (30).

$$\sin\left[2\theta\right] = \frac{2\Delta_{a\gamma\gamma}}{\frac{\sqrt{4\vec{B}_{\mathrm{n}}^2 g_{\mathrm{a}\gamma\gamma}^2 \omega^2 + \left(m_{\mathrm{a}}^2 - \omega_{\mathrm{p}}^2\right)^2}}{4\omega}} \tag{30}$$

Now use the above expressions in (29), as a result, we get a very well simplified form for the axion conversion probability as in (31).

$$P_{a\to\gamma} \simeq \left(g_{\mathrm{a}\gamma\gamma}\vec{B}_{\mathrm{n}}\, t\right)^2 \mathcal{F}\left(\omega, t\right) . \tag{31}$$

Since (32).

$$\mathcal{F}\left(\omega, t\right) = \frac{\sin^2\left[\frac{\sqrt{4g_{\mathrm{a}\gamma\gamma}^2\vec{B}_{\mathrm{n}}^2\omega^2+\left(m_{\mathrm{a}}^2-\omega_{\mathrm{p}}^2\right)^2}}{4\omega}t\right]}{\left(\frac{\sqrt{4g_{\mathrm{a}\gamma\gamma}^2\vec{B}_{\mathrm{n}}^2\omega^2+\left(m_{\mathrm{a}}^2-\omega_{\mathrm{p}}^2\right)^2}}{4\omega}\right)^2} \sim 1 \tag{32}$$

The mass dimension of $\omega_{\mathrm{p}} = \omega = m_{\mathrm{a}} = M^1$, $\vec{B}_{\mathrm{n}} = M^2$ and $g_{\mathrm{a}\gamma\gamma} = t = M^{-1}$, since, conversion probability $P_{a\to\gamma}$ must be dimensionless, in (31) confirms its physical validity and reveals key scaling behaviors. From (31), we derive the scaling of the conversion probability with the physical parameters:

– Magnetic field $\vec{B}_{\mathrm{n}}$: the probability scales as $P_{\mathrm{a}\to\gamma} \propto B_{\mathrm{n}}^2$. In the strong-field regime, the pre-factor saturates to 1, and the probability oscillates sinusoidally.
– Axion mass m_{a}: in the small-mixing regime, $P_{\mathrm{a}\to\gamma} \propto m_{\mathrm{a}}^{-4}$. This strong inverse dependence on the axion mass means that lighter axions have a significantly higher conversion probability in NS magnetospheres for a fixed coupling $g_{\mathrm{a}\gamma\gamma}$.
– Propagation distance (time t): the probability oscillates as $\sin^2\left[\theta t\right]$, this oscillatory behavior with time (which corresponds to propagation distance for a non-relativistic axion) is a hallmark of coherent quantum mixing. The characteristic oscillation length $L_{\mathrm{osc}} = \pi/\kappa$ determines the scale over which the probability cycles from zero to its maximum value. For the simplified case where the axion mass term dominates ($\kappa \simeq m_{\mathrm{a}}^2/(4\omega)$), the oscillation length scales as $L_{\mathrm{osc}} \propto \omega/m_{\mathrm{a}}^2$.

Our state evolution formalism provides a foundational framework that can be integrated with broader astrophysical modeling to enhance its predictive power and testability. A natural extension of this work involves coupling our model with NS population synthesis [52]. By applying our conversion probability to a synthetic population of NS with varying magnetic fields, ages, and distances, we could generate statistically significant predictions for the all-sky flux of axion-induced photons. This would allow for direct comparison with unresolved background radiation in radio and X-ray surveys, setting more robust, population-averaged constraints on axion parameters. Furthermore, our results can be incorporated into spectral modeling codes for individual NS. By calculating the expected axion-conversion photon flux as a function of energy and adding it to standard magnetospheric emission models, we can search for spectral anomalies or excesses that could be attributed to axions. This approach is particularly promising for interpreting data from next-generation X-ray observatories (e.g., Athena) and radio telescopes like the SKA and MeerKAT [9], [45].

3.6. Validity of the adiabatic approximation and non-adiabatic transitions

Our derivation of the conversion probability (31) assumes a homogeneous environment with a constant mixing matrix. However, in a realistic NS magnetosphere, the magnetic field strength $\vec{B}_{\mathrm{n}}$ and plasma frequency ω_{p} are functions of position. The system's evolution is then governed by a position-dependent Hamiltonian $M(r)$. A key question is whether the adiabatic approximation is valid. This approximation holds when the environment changes slowly compared to the system's internal oscillation frequency. The condition for adiabatically is that the mixing angle $\theta(r)$ changes little over an oscillation length L_{osc} as in (33) [33].

$$\gamma = \frac{|d\theta/dr|}{L_{\mathrm{osc}}^{-1}} \ll 1 \tag{33}$$

Where the oscillation length is $L_{\mathrm{osc}} = 2\pi/|\lambda_2 - \lambda_1| = 2\pi/\Delta_{\mathrm{eff}}$, and $\Delta_{\mathrm{eff}} = \sqrt{4\vec{B}_{\mathrm{n}}^2 g_{\mathrm{a}\gamma\gamma}^2\omega^2 + \left(m_{\mathrm{a}}^2 - \omega_{\mathrm{p}}^2\right)^2}/2\omega$ is the eigenvalue difference from our model.

– When adiabatically holds $\gamma \ll 1$: the system smoothly follows an instantaneous mass eigenstate. In this regime, the conversion probability can be calculated using the Landau-Zener formula for level crossing. If the axion passes through a resonance (where $\omega_{\mathrm{p}}(r) \simeq m_{\mathrm{a}}$, making $\Delta_{\mathrm{a}\gamma\gamma} \simeq \Delta_{\mathrm{p}}$), the adiabatic conversion probability can be very high.

– When non-adiabatic transitions dominate ($\gamma \gtrsim 1$): if the magnetic field or plasma density changes abruptly, for instance, near current sheets in the magnetosphere or in turbulent regions, the system cannot adjust smoothly. Non-adiabatic transitions become significant. In the extreme non-adiabatic (sudden) limit, the conversion probability is given by the instantaneous mixing angle at that point, $P_{\mathrm{a}\to\gamma} \sim \sin^2[2\theta]$.

For the magnetospheres of magnetars and pulsars, the gradient of the magnetic field ($d\vec{B}_{\mathrm{n}}/dr \sim \vec{B}_{\mathrm{n}}/R_{\mathrm{NS}}$) is typically very large. Furthermore, the plasma density can have sharp gradients. Our homogeneous model, which yields a constant conversion probability, is most directly applicable to scenarios where non-adiabatic transitions dominate in localized regions, or as a benchmark for the maximum conversion probability in a uniform zone. A comprehensive treatment of the radially inhomogeneous case, including a full analysis of the adiabatic parameter γ, is reserved for future work involving numerical integration of the evolution equations through realistic magnetospheric profiles.

3.7. Advanced magnetospheric effects: quantum electrodynamics birefringence and turbulence

Our model provides a foundational framework using the state evolution formalism. A complete, high-precision description of axion-photon conversion in NS magnetospheres must eventually incorporate two key physical effects. Quantum electrodynamics (QED) vacuum birefringence and magnetospheric turbulence.

3.7.1. Quantum electrodynamics vacuum birefringence

In the presence of ultra-strong magnetic fields ($\vec{B}_{\mathrm{n}} \gtrsim 10^{12}$ G), QED effects become significant. The vacuum behaves as a non-linear medium, leading to vacuum birefringence [53], [54]. This means the photon polarization eigenstates parallel ($\|$) and perpendicular ($\perp$) to the external magnetic field experience different refractive indices. This has a profound impact on axion-photon mixing. The mixing matrix M in (22) must be expanded to a 3×3 form to account for the two-photon polarization states and the axion as in (34).

$$M = \begin{pmatrix} \Delta_{\|} & 0 & \Delta_{\mathrm{a}\gamma}\cos\theta \\ 0 & \Delta_{\perp} & \Delta_{\mathrm{a}\gamma}\sin\theta \\ \Delta_{\mathrm{a}\gamma}\cos\theta & \Delta_{\mathrm{a}\gamma}\sin\theta & \Delta_a \end{pmatrix} \tag{34}$$

Where $\Delta_{\|}$ and $\Delta_{\perp}$ now include contributions from both plasma effects (ω_{p}) and the QED vacuum polarization $\Delta_{\mathrm{QED}} \propto (B/B_{\mathrm{crit}})^2$. The angle θ is between the photon's wave vector and the magnetic field. The strong birefringence can suppress or enhance conversion depending on the photon polarization and the propagation path. For instance, the conversion probability can be resonantly enhanced when the axion mass matches either $\Delta_{\|}$ or $\Delta_{\perp}$, creating more complex resonance structures than in the pure-plasma case.

3.7.2. Magnetospheric turbulence

The assumption of a smooth, stationary magnetosphere is an idealization. Real pulsar and magnetar magnetospheres are dynamic, featuring turbulence, current sheets, and propagating plasma waves [55]–[57]. Turbulence introduces two primary effects:

– Spatial inhomogeneity: turbulent fluctuations in the plasma density $\omega_{\mathrm{p}}(\mathrm{r}, t)$ and magnetic field $B_{\mathrm{n}}(\mathrm{r}, t)$ create a patchy conversion environment. This can lead to localized "hot spots" of axion-photon conversion.
– Non-adiabatic transitions: as discussed in section 3.6, sharp gradients at current sheets or turbulent fronts can violate the adiabatic condition ($\gamma \gtrsim 1$). In these regions, non-adiabatic transitions dominate, and the conversion probability can be approximated by the local, instantaneous mixing angle, $P_{\mathrm{a}\to\gamma} \sim \sin^2(2\theta)$, potentially leading to burst-like or transient photon signals.

In our current model, these effects are not included. Therefore, our results represent a benchmark in the simplified case of a homogeneous, stationary magnetosphere without QED corrections. Future work will integrate these advanced effects, with the state evolution formalism providing a versatile framework for such numerical studies in time-dependent, inhomogeneous backgrounds.

3.8. Flux analysis

We assume that axions can only convert into photons at r_c, where the plasma mass equals the axion mass; otherwise, there is no mixing between axion and photon, and plasma behaves like a mirror. The conversion probability $P_{\mathrm{a}\to\gamma}(t)$ depends on the local magnetic field strength as well as the direction of the axion at that point. The total flux projected from a NS can be expressed in terms of the intensity as follows, $F = \int d\Omega\, n_{\mathrm{a}} v_{\mathrm{a}}\, P_{\mathrm{a}\to\gamma}(t)/4\pi$ [58]. Here, integral over solid angle $d\Omega$ covers the NS and we can express this inter of $dA = D^2 d\Omega$ its physical size is very small and D is the distance between the observer and NS and

numerically $\sim 250\,\mathrm{pc}$. Here, we consider an isotropic distribution of axions in NS, then the intensity of the photon signal is $I(\Omega)$, will be (35).

$$I(\Omega) = \frac{n_{\mathrm{a}}\, v_{\mathrm{a}}}{4\pi} \tag{35}$$

Where n_a is the number of axions, we can write $\rho_{\mathrm{DM}}/m_{\mathrm{a}}$. Here, we assume non-perpendicular emission, But this expression is also valid for axion conversion in the perpendicular case. The expression for the total flux is given by (36).

$$\Phi_{\mathrm{a}\to\gamma} = \int \frac{r^2 \sin(\theta)\, d\theta\, d\phi}{4\pi D^2}\, n_{\mathrm{a}} P_{\mathrm{a}\to\gamma}\, \vec{v}_{\mathrm{DM}} \tag{36}$$

Which leads to the master expression for photon flux as in (37).

$$\Phi_{\mathrm{a}\to\gamma} \simeq \frac{g^2_{\mathrm{a}\gamma\gamma}\rho_{\mathrm{DM}}\vec{B}^2_{\mathrm{n}}\vec{v}_{\mathrm{DM}}\,\mathrm{r}^2 t^2}{D^2 m_{\mathrm{a}}} \tag{37}$$

Here, r is the radius of NS and v_{DM} is the virial velocity [9], [58]. Throughout this letter, the ∞ superscript will show that the value is taken to be that as determined by a distant observer.

4. RADIATED POWER

In the last section, we explored the fact that the conversion probability of axion DM into photons from the state evolution approach is much faster than that from the static state. This is quite surprising, given the correct implementation of the axion signal on earth and the NS cooling rate. The phase-space distribution (PSD) $f(\mathrm{r},\mathrm{v})$, characterizes the statistical properties (spatial positions r and velocities v) of an assembly of particles. Assuming the PSD is stationary leads to Liouville's theorem [59], which expresses that the PSD is conserved laterally by the system's trajectories. Consequently, we can associate the PSD at infinity with the PSD at the surface of the NS is $f(\mathrm{r},\mathrm{v}) = f_\infty(\mathrm{r}_\infty,\mathrm{v}_\infty)$. The distribution of DM is supposed to be isotropic in the rest frame of the galaxy. Then standard halo model predicts an isotropic Maxwellian distribution far from the NS as $f(\mathrm{r},\mathrm{v}) = \rho_{\mathrm{DM}}/\left(2\pi\sigma^2\right)^{3/2} e^{\left(-\mathrm{v}^2/2\sigma^2\right)}$, which becomes (38).

$$f(\mathrm{r}_\infty,\mathrm{v}_\infty) = \frac{\rho^\infty_{\mathrm{DM}}}{\left(2\pi\sigma^2\right)^{3/2}} e^{\left(-\frac{\mathrm{v}^2_\infty}{2\sigma^2}\right)} \tag{38}$$

Here, $2\sigma = v_0$, $\boldsymbol{v}_\infty \approx \sqrt{\boldsymbol{v}(\mathrm{r})^2 - 2GM_{\mathrm{n}}/\mathrm{r}}$ and G and M_{N} are showing Newton's gravitational constant and mass of NS. After the integration of PSD function over $\boldsymbol{v}$ and from $\sqrt{2GM_{\mathrm{n}}/\boldsymbol{r}} \le |\boldsymbol{v}|$, then our expression will be (39).

$$\rho_{\mathrm{DM}}(\boldsymbol{r}) = \frac{2\rho^\infty_{\mathrm{DM}}}{\sqrt{\pi}}\left(\frac{\boldsymbol{v}}{\boldsymbol{v}_\infty} + \int^\infty_{\sqrt{2GM_{\mathrm{n}}/\boldsymbol{r}\boldsymbol{v}^2_0}} e^{-\left(\frac{\boldsymbol{v}}{\boldsymbol{v}_0}\right)^2} d\left(\frac{\boldsymbol{v}}{\boldsymbol{v}_0}\right)\right) \tag{39}$$

And after expansion over $\boldsymbol{v}^2_0/(GM_{\mathrm{n}}/\boldsymbol{r}) \lll 1$, then (40).

$$\rho_{\mathrm{DM}}(\boldsymbol{r}) \simeq \frac{2\rho^\infty_{\mathrm{DM}}}{\sqrt{\pi}\boldsymbol{v}_0}\sqrt{\frac{2GM_{\mathrm{n}}}{\boldsymbol{r}}} \tag{40}$$

The relation for $\boldsymbol{v}(\boldsymbol{r})$ is $\sqrt{2GM_{\mathrm{n}}/\boldsymbol{r}}$ expression for radiated power is $d\mathcal{P}/d\Omega \simeq 2P^\infty_{a\to\gamma}\rho_{\mathrm{DM}}\boldsymbol{v}(\boldsymbol{r})\,\boldsymbol{r}^2$, then our master equation as in (41).

$$\frac{d\mathcal{P}_{\mathrm{SE}}}{d\Omega} \simeq \frac{2\rho^\infty_{\mathrm{DM}}}{\sqrt{\pi}\boldsymbol{v}_0}\frac{2GM_{\mathrm{n}}}{\boldsymbol{r}}\left(g_{\mathrm{a}\gamma\gamma}\vec{B}_{\mathrm{n}}\mathrm{r}\,t\right)^2 \mathcal{F}(\omega,t) \tag{41}$$

We adopt a simplified Goldreich-Julian model for the neutron star magnetosphere [42]. This Goldreich-Julian model provides minimum plasma density required for a self-consistent solution to Maxwell's equations, assuming that particles along magnetic field lines co-rotate with the star. A more realistic model of the neutron star magnetosphere and the axion/photon conversion in this context is also mandatory. However,

from this viewpoint, our approximation should be considered conservative, as the analysis in [44] specified that additional detailed modeling could lead to a stronger signal. Recently, it was proposed that the resonance condition could be extended to light axions, altering the theoretical outline randomly. We also hope the thermal background of a neutron star will be part of a powerful signal of axion power [9]. Figures 3 and 4 shows the sensitivity in $g_{a\gamma\gamma}$ from 100 h of observation of one of the isolated NS, J0806.4-4123. In Figure 3, the blue-violet region is the exclusion region corresponding to the state evolution approach [37].

This NS has a period $R \approx 11.37$s, magnetic field $\vec{B}_{\rm n} \simeq 10^{12}$G, and is at a distance 250 pc from earth [60], [61]. We also assume that NS mass is equal to 1.4 solar masses and r $\simeq$ 10 km. As a result, our expected radiated power for state evolution is $\simeq 3.7 \times 10^{23}$ W. Since this result is 10^{13} times greater than power that expect in laboratories [9].

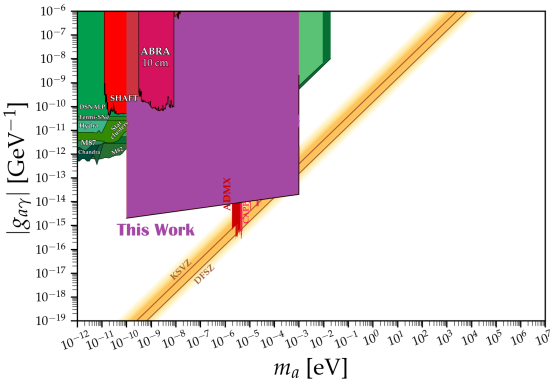

Figure 3. Exclusion contour for the parameters indicated [37]

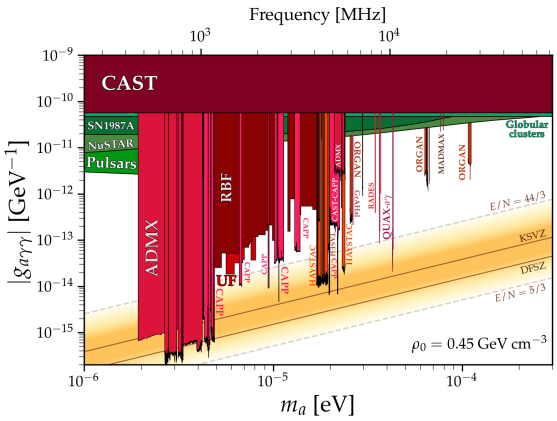

Figure 4. Constraint on axion-photon coupling with mass from different experiments and figure generated via AxionLimits data [62]

5. RESULT AND DISCUSSION

This result is the most significant finding of our study. It indicates that the power emitted via axion-photon conversion, when treated with a time-dependent state evolution approach, is approximately 10^{13} orders of magnitude larger than estimates derived from static or propagating-state formalisms found in the literature [9]. This dramatic enhancement has profound implications:

– Observational prospects: such a powerful signal dramatically improves the prospects for detection with next-generation telescopes. Our model suggests that targeted observations of nearby NS with instruments like the SKA [45], MeerKAT [9], JWST [38], [39], and the Five-hundred-meter Aperture Spherical Telescope (FAST) [63] could probe axion-photon couplings as low as $g_{\rm a\gamma\gamma} \simeq 10^{-15}\,{\rm GeV}^{-1}$ for $m_{\rm a} \simeq 10^{-6}\,{\rm eV}$, venturing into parameter space previously thought to be inaccessible via NS observations.

– NS cooling: this enhanced radiated power represents a strong energy-loss mechanism for the NS. If axions with the considered properties exist, our results imply significantly accelerated NS cooling, as the energy extracted via axion conversion and subsequent photon emission would be substantial. This provides a testable astrophysical constraint consistent with discussions of rapid cooling in certain NS systems [28], [29].
– Comparison with existing work: the predicted radiated power far exceeds the values typically reported in studies using the WKB approximation [31]–[33]. The discrepancy highlights the critical importance of the methodological approach. While previous works often average over non-resonant paths or assume a steady-state propagation, our state evolution method captures the coherent, time-dependent buildup of the photon state, leading to a much higher efficiency for the conversion process.

6. LIMITATIONS AND FUTURE DIRECTIONS

While the model provides a compelling and novel result, we acknowledge its limitations, which also chart a course for future research.

– Homogeneous assumption: our analytical derivation assumes a homogeneous magnetic field and plasma density. As noted in section 3.6, realistic magnetospheres are highly inhomogeneous. Future work involving numerical integration of the evolution equations through realistic magnetospheric profiles (e.g., the Goldreich-Julian model [42]) is essential to refine our predictions.
– QED and turbulence: as discussed in section 3.7, the inclusion of QED vacuum birefringence and magnetospheric turbulence will modify the mixing matrix and potentially suppress or enhance the conversion in complex ways. Incorporating these effects into the state evolution formalism is a critical next step for high-precision predictions.
– Adiabaticity: the validity of the adiabatic approximation needs to be rigorously assessed for specific NS models. In regions with sharp gradients, non-adiabatic transitions will dominate, and our homogeneous result serves as a benchmark for the maximum conversion probability in a uniform zone.

Looking forward, several theoretical extensions of this work present exciting avenues for research.

– Gravitational lensing effects: the intense gravitational field of NS can lens the photons produced via axion conversion. Future models could incorporate ray-tracing in curved spacetime to calculate the resulting amplification and distortion of the observed signal, which could be a distinctive signature.
– Time-dependent magnetospheres: our current analysis assumes a static magnetosphere. A critical next step is to model time-dependent magnetospheres, especially during pulsar glitches or magnetar flares. Such dynamic events could temporarily enhance conversion probabilities, leading to detectable transient signals.
– Coupling to other dark sector particles: the axion may not be an isolated particle but part of a broader "dark sector". Future work could explore scenarios where the axion couples to other DM candidates, such as dark photons or hidden fermions, and investigate how these interactions might modify the conversion phenomenology or produce multi-messenger signals in NS environments.

7. CONCLUSION

This work has developed a state evolution formalism to calculate the axion-photon conversion probability within NS magnetospheres, providing a comprehensive theoretical framework that moves beyond traditional stationary-path approximations. NS, with their extreme gravitational fields, powerful magnetic fields (up to 10^{12} G in magnetars), and dense plasma environments, serve as unique natural laboratories for probing axion physics. In these environments, axions are produced via mechanisms like nucleon-nucleon bremsstrahlung and pionic processes, accumulating over time to form dense axion clouds around the compact objects. By employing the Primakoff effect within our time-dependent state evolution approach, we have derived a new analytical expression for the conversion probability. This formalism, which treats the axion-photon system as a quantum-mechanical two-level system, reveals a conversion probability that is fundamentally different from the scaling found in static approximations. For an axion mass $\left(10^{-3} - 10^{-10}\right)$ eV, our model predicts that NS observations can constrain the axion-photon coupling strength to levels as low as $\left(10^{-14} - 10^{-15}\right)$ GeV^{-1}. The conversion process is significantly influenced by plasma effects through the plasma frequency ω_{p} and the NS's magnetic field geometry, enhancing potentially observable signals such as sharp radio spectral lines and transient electromagnetic emissions. Our analysis demonstrates that the radiated power from axion-photon conversion obtained through the state evolution

approach is approximately 10^{13} orders of magnitude larger than estimates from conventional formalisms. This dramatic enhancement has profound implications for both axion detection strategies and NS astrophysics. The substantial power output suggests that axion conversion could contribute significantly to NS energy loss, potentially explaining rapid cooling rates observed in certain systems. Furthermore, this enhanced signal strength dramatically improves detection prospects with next-generation telescopes, including the SKA, MeerKAT, JWST, GBT, and the FAST. By establishing correlations between key NS parameters, magnetic field strength, rotation rate, age, and the expected axion-induced signals, our work provides a robust framework for interpreting observational data and setting stringent constraints on axion properties, thereby bridging fundamental particle physics with observable astrophysical phenomena.

ACKNOWLEDGMENTS

We thank to Ali Muhammad and Mussawir Khan for their useful discussions on the related topics.

FUNDING INFORMATION

This research was support by the Chinese Government Scholarship (CSC).

AUTHOR CONTRIBUTIONS STATEMENT

This journal uses the Contributor Roles Taxonomy (CRediT) to recognize individual author contributions, reduce authorship disputes, and facilitate collaboration.

Name of Author	C	M	So	Va	Fo	I	R	D	O	E	Vi	Su	P	Fu
Bilal Ahmad	✓	✓	✓	✓	✓	✓	✓	✓	✓	✓	✓	✓	✓	
Shahreyar Ali	✓			✓		✓		✓	✓	✓	✓			

C : **C**onceptualization
M : **M**ethodology
So : **So**ftware
Va : **Va**lidation
Fo : **Fo**rmal Analysis
I : **I**nvestigation
R : **R**esources
D : **D**ata Curation
O : Writing - **O**riginal Draft
E : Writing - Review & **E**diting
Vi : **Vi**sualization
Su : **Su**pervision
P : **P**roject Administration
Fu : **Fu**nding Acquisition

CONFLICT OF INTEREST STATEMENT

The authors state no conflict of interest.

DATA AVAILABILITY

The data that support the findings of this study are available from the corresponding author, [BA], upon reasonable request. The data, which contains information that could compromise the privacy of research participants, is not publicly available due to certain restrictions.

REFERENCES

[1] R. D. Peccei and H. R. Quinn, "Constraints imposed by CP conservation in the presence of pseudoparticles," *Physical Review D*, vol. 16, no. 6, pp. 1791–1797, 1977, doi: 10.1103/PhysRevD.16.1791.
[2] S. Weinberg, "A new light boson?," *Physical Review Letters*, vol. 40, no. 4, pp. 223–226, 1978, doi: 10.1103/PhysRevLett.40.223.
[3] F. Wilczek, "Problem of strong P and T invariance in the presence of instantons," *Physical Review Letters*, vol. 40, no. 5, pp. 279–282, 1978, doi: 10.1103/PhysRevLett.40.279.
[4] G. 'T Hooft, "Symmetry breaking through Bell-Jackiw anomalies," *Physical Review Letters*, vol. 37, no. 1, pp. 8–11, 1976, doi: 10.1103/PhysRevLett.37.8.
[5] P. Svrček and E. Witten, "Axions in string theory," *Journal of High Energy Physics*, vol. 2006, 2006, doi: 10.1088/1126-6708/2006/06/051.
[6] A. Arvanitaki, S. Dimopoulos, S. Dubovsky, N. Kaloper, and J. M.- Russell, "String axiverse," *Physical Review D*, vol. 81, no. 12, 2010, doi: 10.1103/PhysRevD.81.123530.
[7] P. Sikivie, "Experimental tests of the 'invisible' axion," *Physical Review Letters*, vol. 51, no. 16, pp. 1415–1417, 1983, doi: 10.1103/PhysRevLett.51.1415.

[8] J. N. Bahcall and R. A. Wolf, "Neutron stars. I. Properties at absolute zero temperature," *Physical Review*, vol. 140, no. 5B, pp. B1445–B1451, Dec. 1965, doi: 10.1103/PhysRev.140.B1445.
[9] Y. F. Zhou *et al.*, "Searching for axion dark matter with the MeerKAT radio telescope," *Physical Review D*, vol. 106, no. 8, 2022, doi: 10.1103/PhysRevD.106.083006.
[10] J. D. Miguel, "Retuning radio astronomy for axion dark matter with neutron stars," *Physics Letters, Section B: Nuclear, Elementary Particle and High-Energy Physics*, vol. 862, 2025, doi: 10.1016/j.physletb.2025.139328.
[11] M. E. Gusakov, E. M. Kantor, and D. D. Ofengeim, "Evolution of the magnetic field in neutron stars," *Physical Review D*, vol. 96, no. 10, 2017, doi: 10.1103/PhysRevD.96.103012.
[12] M. K. Liou, "Low-energy theorem for nucleon-nucleon bremsstrahlung," *Physical Review C*, vol. 2, no. 1, pp. 131–138, 1970, doi: 10.1103/PhysRevC.2.131.
[13] M. Giannotti and F. Nesti, "Nucleon-nucleon bremsstrahlung emission of massive axions," *Physical Review D*, vol. 72, no. 6, 2005, doi: 10.1103/PhysRevD.72.063005.
[14] T. Fischer, P. Carenza, B. Fore, M. Giannotti, A. Mirizzi, and S. Reddy, "Observable signatures of enhanced axion emission from protoneutron stars," *Physical Review D*, vol. 104, no. 10, 2021, doi: 10.1103/PhysRevD.104.103012.
[15] B. Ahmad, Y.-A. Liu, and N. Houston, "Resonant enhancement of axion dark matter decay," 2025, *arXiv:2507.18508*.
[16] M. S. Pshirkov and S. B. Popov, "Conversion of dark matter axions to photons in magnetospheres of neutron stars," *Journal of Experimental and Theoretical Physics*, vol. 108, no. 3, pp. 384–388, 2009, doi: 10.1134/S1063776109030030.
[17] D. Noordhuis, A. Prabhu, C. Weniger, and S. J. Witte, "Axion clouds around neutron stars," *Physical Review X*, vol. 14, no. 4, 2024, doi: 10.1103/PhysRevX.14.041015.
[18] H. Primaxofpf, "Photo-production of neutral mesons in nuclear electric fields and the mean life of the neutral meson," *Physical Review*, vol. 80, pp. 580–594, 1950.
[19] M. Kawasaki, K. Saikawa, and T. Sekiguchi, "Axion dark matter from topological defects," *Physical Review D*, vol. 91, no. 6, doi: 10.1103/PhysRevD.91.065014.
[20] R. T. Co, L. J. Hall, and K. Harigaya, "Axion kinetic misalignment mechanism," *Physical Review Letters*, vol. 124, no. 25, 2020, doi: 10.1103/PhysRevLett.124.251802.
[21] S. Chang, C. Hagmann, and P. Sikivie, "Studies of the motion and decay of axion walls bounded by strings," *Physical Review D* , vol. 59, no. 2, 1998, doi: 10.1103/PhysRevD.59.023505.
[22] A. Ringwald and K. Saikawa, "Axion dark matter in the post-inflationary Peccei-Quinn symmetry breaking scenario," *Physical Review D*, vol. 93, no. 8, 2016, doi: 10.1103/PhysRevD.93.085031.
[23] A. H. Guth, "Inflationary universe: a possible solution to the horizon and flatness problems," Physical Review D, vol. 23, no. 2, pp. 347–356, 1981, doi: 10.1103/PhysRevD.23.347.
[24] D. H. Lyth and E. D. Stewart, "Axions and inflation: string formation during inflation," *Physical Review D*, vol. 46, no. 2, pp. 532–538, 1992, doi: 10.1103/PhysRevD.46.532.
[25] S. M. Barr and D. Hochberg, "Fine structure of local and axion strings," *Physical Review D*, vol. 39, no. 8, pp. 2308–2316, 1989, doi: 10.1103/PhysRevD.39.2308.
[26] M. C. Huang and P. Sikivie, "Structure of axionic domain walls," *Physical Review D*, vol. 32, no. 6, pp. 1560–1568, 1985, doi: 10.1103/PhysRevD.32.1560.
[27] M. S. Turner and F. Wilczek, "Inflationary axion cosmology," *Physical Review Letters*, vol. 66, no. 1, pp. 5–8, Jan. 1991, doi: 10.1103/PhysRevLett.66.5.
[28] S. Han and A. W. Steiner, "Cooling of neutron stars in soft X-ray transients," *Physical Review C*, vol. 96, no. 3, 2017, doi: 10.1103/PhysRevC.96.035802.
[29] D. Blaschke, H. Grigorian, D. N. Voskresensky, and F. Weber, "Cooling of the neutron star in Cassiopeia A," *Physical Review C*, vol. 85, no. 2, 2012, doi: 10.1103/PhysRevC.85.022802.
[30] D. Noordhuis, A. Prabhu, C. Weniger, and S. J. Witte, "Axion clouds around neutron stars," *Physical Review X*, vol. 14, no. 4, 2024, doi: 10.1103/PhysRevX.14.041015.
[31] H. Terças, J. T. Mendonça, and R. Bingham, "Resonant axion-plasmon conversion in neutron star magnetospheres," *Physical Review Letters*, vol. 135, no. 11, Sep. 2025, doi: 10.1103/5hbb-yy48.
[32] D. Noordhuis, A. Prabhu, C. Weniger, and S. J. Witte, "Axion clouds around neutron stars," *Physical Review X*, vol. 14, no. 4, 2024, doi: 10.1103/PhysRevX.14.041015.
[33] A. Hook, Y. Kahn, B. R. Safdi, and Z. Sun, "Radio signals from axion dark matter conversion in neutron star magnetospheres," *Physical Review Letters*, vol. 121, no. 24, 2018, doi: 10.1103/PhysRevLett.121.241102.
[34] L. B. Leinson, "Axion mass limit from observations of the neutron star in Cassiopeia A," *Journal of Cosmology and Astroparticle Physics*, vol. 2014, no. 8, 2014, doi: 10.1088/1475-7516/2014/08/031.
[35] E. F. Brown, A. Cumming, F. J. Fattoyev, C. J. Horowitz, D. Page, and S. Reddy, "Rapid neutrino cooling in the neutron star MXB 1659-29," *Physical Review Letters*, vol. 120, no. 18, 2018, doi: 10.1103/PhysRevLett.120.182701.
[36] J. W. Foster *et al.*, "Green bank and effelsberg radio telescope searches for axion dark matter conversion in neutron star magnetospheres," *Physical Review Letters*, vol. 125, no. 17, Oct. 2020, doi: 10.1103/PhysRevLett.125.171301.
[37] R. A. Battye, M. J. Keith, J. I. McDonald, S. Srinivasan, B. W. Stappers, and P. Weltevrede, "Searching for time-dependent axion dark matter signals in pulsars," *Physical Review D*, vol. 108, no. 6, 2023, doi: 10.1103/PhysRevD.108.063001.
[38] S. Roy, C. Blanco, C. Dessert, A. Prabhu, and T. Temim, "Sensitivity of JWST to eV-Scale decaying axion dark matter," *Physical Review Letters*, vol. 134, no. 7, 2025, doi: 10.1103/PhysRevLett.134.071003.
[39] R. Janish and E. Pinetti, "Hunting dark matter lines in the infrared background with the James webb space telescope," *Physical Review Letters*, vol. 134, no. 7, 2025, doi: 10.1103/PhysRevLett.134.071002.
[40] M. P. Van Haarlem *et al.*, "LOFAR: the low-frequency array," *Astronomy and Astrophysics*, vol. 556, 2013, doi: 10.1051/0004-6361/201220873.
[41] GBT Support Staff, *The proposer's guide for the Green Bank telescope*. Green Bank, United States: Green Bank Observatory, 2008.
[42] P. Goldreich and W. H. Julian, "Pulsar electrodynamics," *The Astrophysical Journal*, vol. 157, Aug. 1969, doi: 10.1086/150119.

[43] J. Hecht, N. Potter, and M. Koziol, "Inside the universe machine: IEEE spectrum explores the webb telescope's groundbreaking engineering," *IEEE Spectrum*, vol. 59, no. 9, pp. 22–30, 2022, doi: 10.1109/MSPEC.2022.9881257.
[44] S. J. Witte, D. Noordhuis, T. D. P. Edwards, and C. Weniger, "Axion-photon conversion in neutron star magnetospheres: The role of the plasma in the Goldreich-Julian model," *Physical Review D*, vol. 104, no. 10, 2021, doi: 10.1103/PhysRevD.104.103030.
[45] A. Weltman *et al.*, "Fundamental physics with the square kilometre array," *Publications of the Astronomical Society of Australia*, vol. 37, 2020, doi: 10.1017/pasa.2019.42.
[46] C. M. Adair *et al.*, "Search for dark matter axions with CAST-CAPP," *Nature Communications*, vol. 13, no. 1, Oct. 2022, doi: 10.1038/s41467-022-33913-6.
[47] V. C. Rubin and J. W. K. Ford, "Rotation of the andromeda nebula from a spectroscopic survey of emission regions," *The Astrophysical Journal*, vol. 159, 1970.
[48] J. P. Ostriker, P. J. E. Peebles, and A. Yahil, "The size and mass of galaxies, and the mass of the universe," *The Astrophysical Journal*, vol. 193, 1974, doi: 10.1086/181617.
[49] P. Sikivie, D. B. Tanner, and K. V. Bibber, "Resonantly enhanced axion-photon regeneration," *Physical Review Letters*, vol. 98, no. 17, 2007, doi: 10.1103/PhysRevLett.98.172002.
[50] E. Masaki, A. Aoki, and J. Soda, "Photon-axion conversion, magnetic field configuration, and polarization of photons," *Physical Review D*, vol. 96, no. 4, 2017, doi: 10.1103/PhysRevD.96.043519.
[51] G. Raffelt and L. Stodolsky, "Mixing of the photon with low-mass particles," *Physical Review D*, vol. 37, no. 5, pp. 1237–1249, 1988, doi: 10.1103/PhysRevD.37.1237.
[52] U. Bhura, R. Battye, J. McDonald, and S. Srinivasan, "Axion signals from neutron star populations," *Journal of Cosmology and Astroparticle Physics*, no. 11, 2024, doi: 10.1088/1475-7516/2024/11/029.
[53] L. Maiani, R. Petronzio, and E. Zavattini, "Effects of nearly massless, spin-zero particles on light propagation in a magnetic field," *Physics Letters B*, vol. 175, no. 3, pp. 359–363, 1986, doi: 10.1016/0370-2693(86)90869-5.
[54] N. Ahmadiniaz *et al.*, "Detection schemes for quantum vacuum diffraction and birefringence," *Physical Review D*, vol. 108, no. 7, 2023, doi: 10.1103/PhysRevD.108.076005.
[55] M. Imbrogno, C. Meringolo, A. C.- Osorio, L. Rezzolla, B. Cerutti, and S. Servidio, "Turbulence and magnetic reconnection in relativistic multispecies plasmas," *The Astrophysical Journal Letters*, vol. 990, no. 2, 2025, doi: 10.3847/2041-8213/adfb4c.
[56] J. Pétri, "Theory of pulsar magnetosphere and wind," *Journal of Plasma Physics*, vol. 82, no. 5, 2016, doi: 10.1017/s0022377816000763.
[57] P. Guio and H. L. Pécseli, "The Impact of Turbulence on the Ionosphere and Magnetosphere," *Frontiers in Astronomy and Space Sciences*, vol. 7, 2021, doi: 10.3389/fspas.2020.573746.
[58] M. Leroy, M. Chianese, T. D. P. Edwards, and C. Weniger, "Radio signal of axion-photon conversion in neutron stars: a ray tracing analysis," *Physical Review D*, vol. 101, no. 12, 2020, doi: 10.1103/PhysRevD.101.123003.
[59] J. Liouville, "Note sur la Théorie de la Variation des constantes arbitraires," *Journal de Mathématiques Pures et Appliquées*, vol. 3, pp. 342-349, 1838.
[60] C. Kouvaris, T. Liu, and K. F. Lyu, "Radio signals from axion star-neutron star binaries," *Physical Review D*, vol. 109, no. 2, 2024, doi: 10.1103/PhysRevD.109.023008.
[61] D. L. Kaplan and M. H. V. Kerkwijk, "Constraining the spin-down of the nearby isolated neutron star RX J0806.4-4123, and implications for the population of nearby neutron stars," *Astrophysical Journal*, vol. 705, no. 1, pp. 798–808, 2009, doi: 10.1088/0004-637X/705/1/798.
[62] C. O'hare, "AxionLimits: data, plots and code for constraints on axions, axion-like particles, and dark photons," Cajohare GitHub, 2020. [Online]. Available: https://cajohare.github.io/AxionLimits/
[63] R. Nan *et al.*, "The five-hundred-meter aperture spherical radio telescope (FAST) project," *International Journal of Modern Physics D*, vol. 20, no. 06, pp. 989–1024, Jun. 2011, doi: 10.1142/S0218271811019335.

BIOGRAPHIES OF AUTHORS

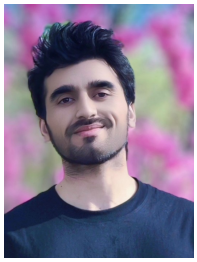

Bilal Ahmad graduated with a bachelor's degree in physics and is currently working as a Ph.D. scholar at Beijing University of Technology, Beijing, China. His research interests include axion physics, dark photon dark matter, and physics beyond the standard model. He can be contacted at email: bilalahmad@emails.bjut.edu.cn.

Shehreyar Ali completed a B.S. degree in Physics from Govt Degree College No 2 Mardan, affiliated with Abdul Wali Khan University Mardan (AWKUM), KPK, Pakistan in 2024, and currently enrolled in Quaid-e-Azam University, Islamabad, Pakistan. His research interests include theoretical physics, high energy physics, axion physics, and neutrino physics. He can be contacted at email: shehreyarkhan675@gmail.com.